Decoupling of Dual-Band Dual-Polarized Base Station Array Antenna

Xuekang Liu
University of Kent
Canterbury, UK
xl255@kent.ac.uk

Steven Gao
University of Kent
Canterbury, UK

Benito Sanz-Izquierdo
University of Kent
Canterbury, UK

Haiwei Zhang
Huawei Technologies Ltd
Shenzhen, China

***Abstract*—Dual-band dual-polarized arrays (DBDPA) using interleaved configuration have drawn industry attention as a promising way to improve channel capacity in a package that has a minimum width. By integrating high-performance filtering elements, a novel interleaved DBDPA for base station use is presented in this paper. For the first time, a radiation null is introduced into the low-band (LB) antenna using the intrinsic suppression mode of folded dipole. Then, to enhance the gain-suppression level in out-of-band to 16 dB, four rectangular loops are introduced under the radiator. To achieve high selectivity for high-band (HB) antenna, a meander line loop is introduced and analyzed for the first time in this paper. Simulations indicate that the presented HB antenna achieves 17 dB of out-of-band rejection and 243 dB/GHz of roll-off rate. The combined use of these two filtering elements finally enables the realization of a DBDPA with low mutual coupling and low cross-band scattering. According to the measurements, this antenna covers two wide frequency ranges of 2.26- 2.73 GHz and 2.98-4.3 GHz with a 25 dB cross-band isolation level.**

Keywords—Decoupling, base station, low frequency ratio, wideband

I. Introduction

In recent years, more and more frequency bands are being developed to satisfy the growing need of information exchange for people. As a result, the dual/multi-band base station array antenna design becomes a new research focus. [1]-[2]. Due to space restrictions, the HB and LB elements of a DBDPA normally share the same radiation aperture and are located near together. As a result of the cross-band scattering and mutual coupling between these elements, the entire array will suffer serious performance degradation.

To solve this problem, many innovative methods are presented in [3]-[12]. A patch antenna with dual-polarizations was presented in [4] to serve two separate frequency ranges. Then, by combining four identical elements, a DBDPA was presented. Although employing a single antenna to cover two frequency bands can significantly simplify the complexity of the feeding network, it is not suitable for arrays with different LB and HB element numbers. By placing the HB antennas above a LB antenna and inserting a layer of split PEC plane between them, a DBDPA that can cover 0.69- 0.96 GHz and 3.5 – 4.9 GHz was achieved in [5]. The split PEC plane performs the function of a reflector for the HB elements. The high frequency electromagnetic wave will be reflected back. Thus, the isolations between the elements in different frequency bands can be developed to 30 dB. However, the frequency ratio of the two frequency bands in this design is larger than 5. Two dual-band dual-polarized array antennas were presented by using filtering elements in [9] and [10]. In these designs, the LB and HB element are expected to obtain low-pass and high-pass response, respectively. Then, by combining these well designed filtering antennas, a interleaved DBDPA can be realized without using any other decoupling structures.

This work was supported in part by EPSRC under Grant EP/S005625/1 and EP/N032497/1, in part by Huawei Technologies Ltd, and in part by China Scholarship Council.

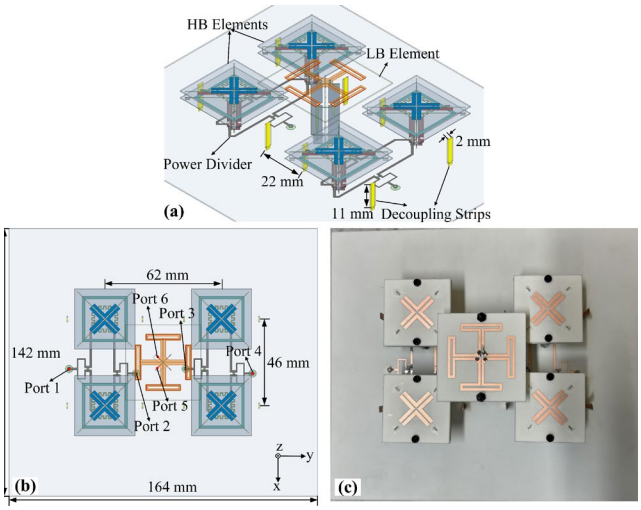

Fig. 1. (a), (b) configurations of the interleaved DBDPA, and (c) fabricated prototype.

In this paper, a novel interleaved DBDPA with low cross-band scattering and low mutual coupling is designed for base station applications. Based on the radiation mode and suppression mode of the folded-dipole antenna, a high selectivity LB element is developed first. Then, by using parasitic loops, a HB antenna with high roll-off rate, broad operating bandwidth, and high gain-suppression level at out-of-band is achieved. Utilizing these well-designed filtering antennas, the cross-band isolation can be improved to above 25 dB without using any other decoupling structures. Besides, the radiation performance of the HB array maintains almost the same with and without LB element due to the inherent low scattering feature of the presented LB antenna..

II. Design of DBDPA

Fig. 1 shows the configurations of the proposed DBDPA. There are five antennas in the proposed design: a HB element and four HB element. The four HB elements are arranged around the LB element, which is at the centre of the array. Four power dividers are used to fed the eight ports of the HB antennas. As shown in Fig. 1(b), the distances between the HB elements are different along different axes. All the substrates in this design are Rogers 4003 substrates ($\tan\delta = 0.0027$, $\varepsilon_r =$

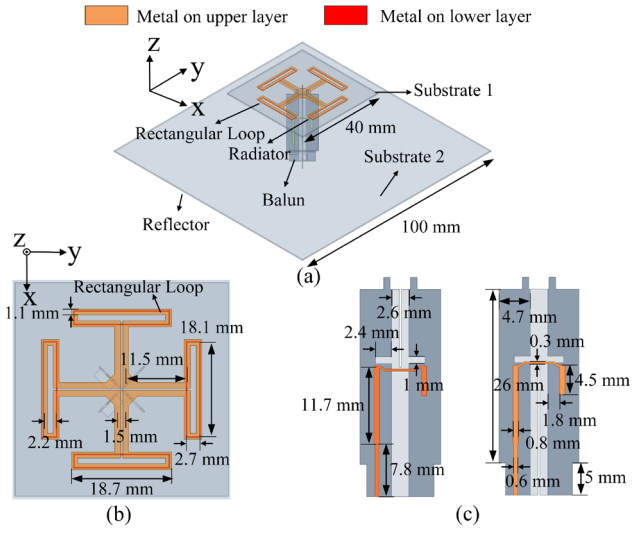

Fig. 2. Configurations and detailed dimensions of the LB filtering element.

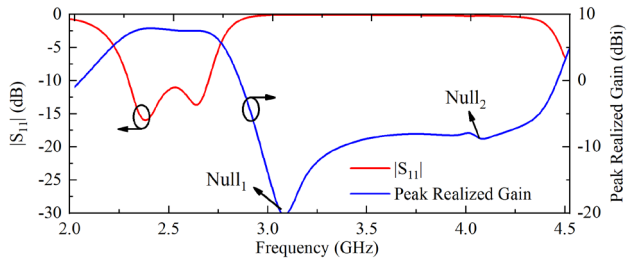

Fig. 3. Simulated results of the LB element.

3.55). The detailed dimensions and working principles of each element will be given in the follow sub-sections. The commercial electromagnetic simulation software Ansys HFSS was used to conduct all of the simulations in this work.

A. LB Filtering Antenna

As can be seen in Fig. 2, the radiator of the LB filtering antenna can be divided into two parts: main radiator and parasitic loops. Both of them are printed on the substrate 1. Substrate 1 and 2 both have a thickness of 0.508 mm. The substrates on the baluns have a thickness of 0.305 mm.

The simulated peak realized gain of the LB antenna and its simulated $|S_{11}|$ are given in Fig. 3. As observed, the proposed work realises a 16 dB rejection level at upper out-of-band and a broad operating bandwidth that can cover the desired band (2.3 GHz- 2.7 GHz). To have a deeper insight into the working principle of this antenna, simulated current distributions of the presented antenna at 2.5 GHz (in-band), 3.1 GHz (out-of-band), and 4.0 GHz (out-of-band) are given in Fig. 4. As shown in Fig. 4(a), point A, B, C, and D are the nulls of the current. It means that the radiator can be seen as disconnected at these points. Thus, the radiator can be divided into four equal parts. Due to the composite current vector on these four parts is along -45° direction, the electromagnetic wave can be transmitted into free space at this frequency (radiation mode). At 3.1 GHz, it can be observed from the current distribution that point A, B, C, and D are the maximum point of the current. The radiator can be seen as shorted transmission line. All the power will be reflected back to the input port (suppression mode). Thus, there will be a radiation null at this frequency. At 4.0 GHz, the currents on the radiator and the rectangular loops flow in the opposite direction, as given in Fig. 4(c).

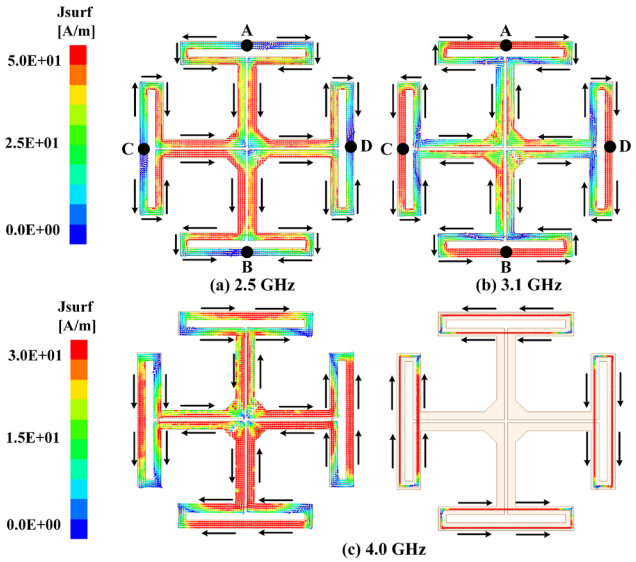

Fig. 4. Simulated J_{surf} of the LB element at different frequencies.

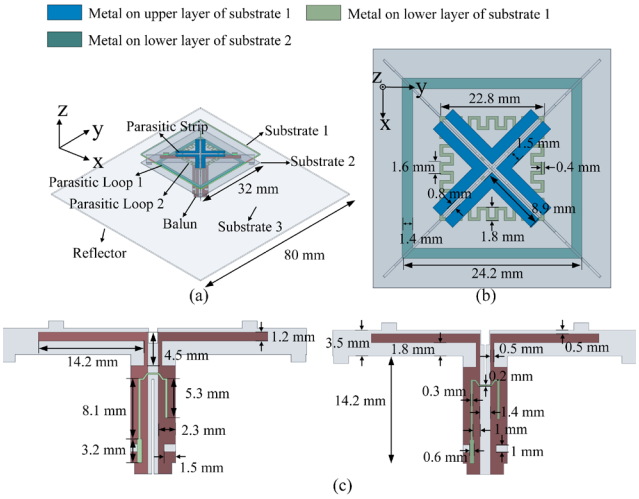

Fig. 5. Configurations and detailed dimensions of the HB filtering element.

Their far-field radiation counteracts each other. Therefore, another radiation null can be obtained.

B. HB Filtering Antenna

Fig. 5 shows the configurations and detailed dimensions of the HB filtering antenna. The main radiators of this antenna are the crossed dipoles printed on the same plane with the baluns. The parasitic loops (parasitic loop 1 and 2) are printed on two different substrates (substrate 2 and substrate 1) and placed below and above the dipole arms of the crossed dipoles, respectively. The thicknesses of substrate 1, 2, and 3 are 0.508 mm, 0.305mm, and 0.508 mm.

The simulated peak realized gain of the HB antenna and its $|S_{11}|$ are depicted in Fig. 6. Simulations show that the presented design can cover a wide frequency range of 42.5% (3.0- 4.62 GHz) with the reference of $|S_{11}| < -14$ dB. Besides, a stable in-band peak realized gain, two radiation nulls, a 17 dB gain-suppression level is also obtained at lower out-of-band Apart from these advantages, the proposed HB element also realizes a high roll-off rate of 243 dB / GHz, which can be calculated by using the calculation method in [13].

By introducing parasitic loop 1, the radiation null 1 can be obtained firstly to suppress the out-of-band radiation [14].

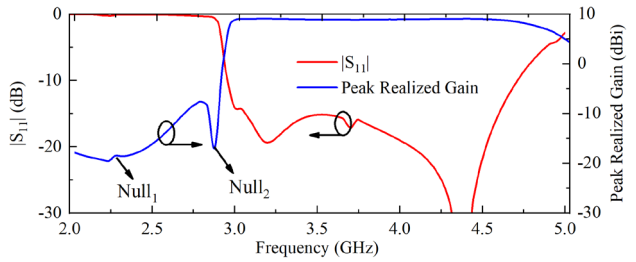

Fig. 6. Simulated results of the HB element.

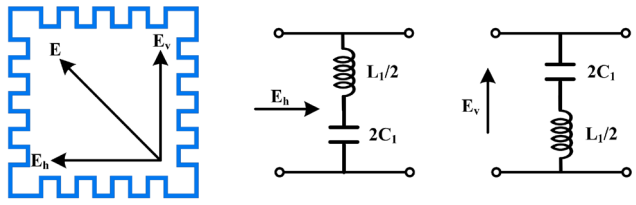

Fig. 7. Equivalent circuit of the parasitic loop 2.

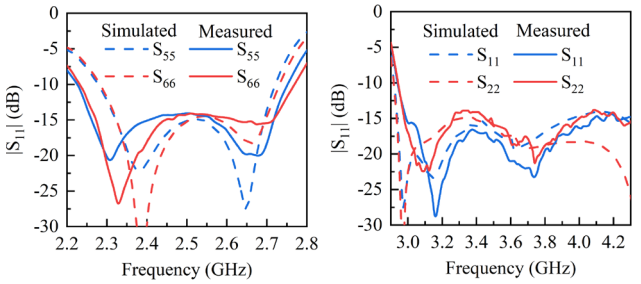

Fig. 8. Comparison of simulated and measured $|S_{11}|$ of the interleaved DBDPA.

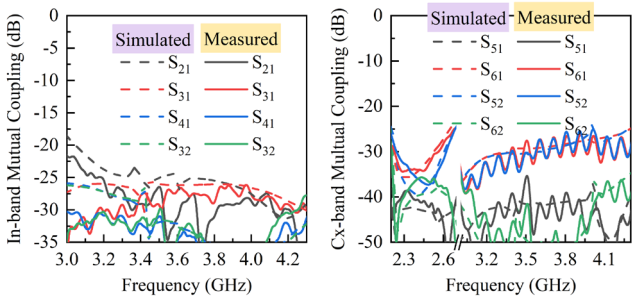

Fig. 9. Comparison of simulated and measured in-band and cross-band mutual couplings of the interleaved DBDPA.

Then, by placing the parasitic loop 2 above the dipole arms, the radiation null 2 is realized to enhance the *RoR* of this antenna. Fig. 7 depicts an equivalent circuit that may be used to understand the working principle of the parasitic loop 2. For different incident EM waves, the meander line structure will act as different elements (capacitance or inductance) [15]. As a result, the parasitic loop 2 function as a series L-C resonator for incident waves with ± 45° polarizations. It will act as a band-stop filter. Therefore, a radiation null can be introduced at its resonant frequency.

III. Results and Discussion

A prototype of the presented interleaved DBDPA is fabricated and measured in order to validate the design principle. R&S®ZVL vector network analyzer and anechoic chamber at University of Kent are used to get the S-parameters and far-field data. As shown in Fig. 8, the proposed interleaved DBDPA can cover a wide LB frequency range of 2.26 GHz- 2.73 GHz and a HB frequency range of 2.98 GHz-4.3 GHz. Both simulated and measured $|S_{11}|$ are lower than -14 dB within these bands. Fig. 9 shows the comparison of simulated and measured mutual couplings of DBDPA. The measurements confirm that the in-band couplings in HB are are below -22 dB. This value is a little bit lower than the simulated one. The measured cross-band isolations of the interleaved DBDPA are higher than 25 dB, which is same as the simulated result. Fig. 10 depicts the realized gains of the interleaved DBDPA at LB and HB. As observed, the measured realized gain varies from 8.6 dBi to 9.2 dBi at LB. And, an average realized gain of 10 dBi is achieved when HB sub-array works.

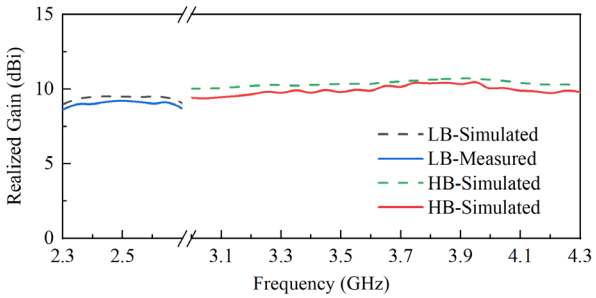

Fig. 10. Comparison of simulated and measured realized gain of the LB element and HB sub-array.

TABLE I
Comparison of the Previously Presented Antennas

Ref.	Elements Arrangement	Imp. BW	$\|S_{11}\|$ (dB)	Freq. Ratio	Cx-band Iso. (dB)
[9]	A HB under LB	2.5-2.7 (7.7%) 3.3-3.8 (14%)	-15	1.37	27
[10]	Side by side	1.65-1.88 (13%) 1.89-2.22 (16%)	-10	1.16	25
[16]	2×2 HB under LB	1.71-2.17 (24%) 3.3-3.8 (14%)	-11	1.8	20
This Work	**2×2 HB under LB**	**2.26-2.73 (19%) 3.0-4.3 (36%)**	**-14**	**1.46**	**25**

Table I shows the comparison of the presented interleaved DBDPA with other previously published works. Although the designs in [9] and [10] obtain a smaller frequency ratio than our proposed one, their impedance bandwidth are much narrower than our work. The impedance bandwidth of the LB element in [16] is wider than the proposed LB antenna. However, the reference level of $|S_{11}|$ in that work is -11 dB. Besides, our presented work realize a smaller frequency ratio and a higher cross-band isolation level than the DBDPA in [16].

IV. Conclusion

By elaborately utilizing the radiation mode and suppression mode of the folded dipole antenna, a broadband dual-polarized antenna with high-stop response and high out-of-band rejection level can be obtained. Besides, a new design technique is demonstrated to realize a dual-polarized filtering antenna with low-stop response and broad operating bandwidth. Based on the presented high-stop LB antenna and low-stop HB antenna, a interleaved DBDPA with low mutual couplings and can be achieved. According to the measured results, a high cross-band isolation level is achieved within two wide frequency ranges. Such a high-performance antenna is a favourable choice for mobile communications base station applications.

REFERENCES

[1] Y. He, Y. Yue, L. Zhang and Z. N. Chen, "A dual-broadband dual-polarized directional antenna for all-spectrum access base station applications," *IEEE Trans. Antennas Propag*., vol. 69, no. 4, pp. 1874-1884, April 2021.

[2] R. Wu and Q. -X. Chu, "A compact, dual-polarized multiband array for 2G/3G/4G base stations, " *IEEE Trans. Antennas Propag*., vol. 67, no. 4, pp. 2298-2304, April 2019.

[3] L. Zhao, K. -W. Qian and K. -L. Wu, "A cascaded coupled resonator decoupling network for mitigating interference between two radios in adjacent frequency bands, " *IEEE Trans. Microw. Theory Techn.*, vol. 62, no. 11, pp. 2680-2688, Nov. 2014.

[4] C. -X. Mao, S. Gao, Y. Wang, Q. Luo and Q. -X. Chu, "A shared-aperture dual-band dual-polarized filtering-antenna-array with improved frequency response, " *IEEE Trans. Antennas Propag*., vol. 65, no. 4, pp. 1836-1844, April 2017.

[5] Y. Chen, J. Zhao and S. Yang, "A novel stacked antenna configuration and its applications in dual-band shared-aperture base station antenna array designs, " *IEEE Trans. Antennas Propag*., vol. 67, no. 12, pp. 7234-7241, Dec. 2019.

[6] Y. Liu, S. Wang, N. Li, J. -B. Wang and J. Zhao, "A compact dual-band dual-polarized antenna with filtering structures for sub-6 GHz base station applications, " *IEEE Antennas Wireless Propag. Lett.*, vol. 17, no. 10, pp. 1764-1768, Oct. 2018.

[7] M. Li, Q. Li, B. Wang, C. Zhou and S. Cheung, "A miniaturized dual-band base station array antenna using band notch dipole antenna elements and AMC reflectors, " *IEEE Trans. Antennas Propag*., vol. 66, no. 6, pp. 3189-3194, June 2018.

[8] X. Zhang, D. Xue, L. Ye, Y. Pan and Y. Zhang, "Compact dual-band dual-polarized interleaved two-beam array with stable radiation pattern based on filtering elements, " *IEEE Trans. Antennas Propag*., vol. 65, no. 9, pp. 4566-4575, Sept. 2017.

[9] S. J. Yang, W. Duan, Y. Y. Liu, H. Ye, H. Yang and X. Y. Zhang, "Compact dual-band base-station antenna using filtering elements, " *IEEE Trans. Antennas Propag*., early access.

[10] M. Li, R. Wang, J. M. Yasir and L. Jiang, "A miniaturized dual-band dual-polarized band-notched slot antenna array with high isolation for base station applications, " *IEEE Trans. Antennas Propag*., vol. 68, no. 2, pp. 795-804, Feb. 2020.

[11] W. Duan, Y. F. Cao, Y. -M. Pan, Z. X. Chen and X. Y. Zhang, "Compact dual-band dual-polarized base-station antenna array with a small frequency ratio using filtering elements, " *IEEE Access*., vol. 7, pp. 127800-127808, 2019.

[12] Y. Zhang, X. Y. Zhang, L. Ye and Y. Pan, "Dual-band base station array using filtering antenna elements for mutual coupling suppression, " *IEEE Trans. Antennas Propag*., vol. 64, no. 8, pp. 3423-3430, Aug. 2016.

[13] X. Liu et al., "A compact dual-polarized filtering antenna with steep cut-off for base-station applications," *IEEE Trans. Antennas Propag*., early access.

[14] C. F. Ding, X. Y. Zhang, Y. Zhang, Y. M. Pan and Q. Xue, "Compact broadband dual-polarized filtering dipole antenna with high selectivity for base-station applications," *IEEE Trans. Antennas Propag.*, vol. 66, no. 11, pp. 5747–5756, Nov. 2018.

[15] B. A. Munk, *Frequency selective surfaces*. New York: Wiley, 2000.

[16] S. J. Yang, R. Ma and X. Y. Zhang, "Self-decoupled dual-band dual-polarized aperture-shared antenna array," *IEEE Trans. Antennas Propag.*, early access.